Potential weakly interacting massive particle signature for the caustic ring halo model

Anne M. Green
Astronomy Unit, School of Mathematical Sciences, Queen Mary University of London, Mile End Road, London, E1 4NS, United Kingdom
(Received 18 December 2000; published 25 April 2001)

Weakly interacting massive particle (WIMP) direct detection event rate calculations usually rely on fairly simple, essentially static, analytic halo models. This is largely since the resolution of numerical simulations is not yet large enough to allow the full numerical calculation of the WIMP density and velocity distribution. In this paper we study the direct detection rate, in particular its energy dependence and annual modulation, for the caustic ring halo model. In this model, which uses simple assumptions to model the infall of dark matter onto the halo, the distribution of the cold dark matter particles at the Earth's location has a series of peaks in velocity space. We find that the recoil energy spectrum contains distinctive steps and the sign of the annual modulation in the event rate changes as a function of recoil energy. These effects provide a potentially distinctive experimental signal.

DOI: 10.1103/PhysRevD.63.103003 PACS number(s): 98.70.Vc, 98.80.Cq

I. INTRODUCTION

Weakly interacting massive particle (WIMP) direct detection experiments are just reaching the sensitivity required to probe the interesting range of mass–cross-section parameter space where relic neutralinos could constitute the dark matter. The DAMA Collaboration, using a detector consisting of radiopure NaI crystal scintillators at the Gran Sasso Laboratory, have reported the detection of a 4σ annual modulation signal in their direct detection experiment, consistent with WIMP scattering [1,2]. Whilst this result is somewhat controversial [3,4] it illustrates the potential of current and upcoming WIMP direct detection experiments.

Event rate calculations and detection strategies for particle physics dark matter candidates are usually based on the assumption of a standard Maxwellian halo model [5–7]. The standard Maxwellian halo model has a number of deficiencies, in particular the real halo contains substructure and is not perfectly spherical and isotropic [8]. Since the resolution of numerical simulations is not yet large enough to allow the full numerical calculation of the WIMP density and velocity distribution, analytic, or at least semianalytic, models for the dark matter halo must be used. The direct detection rate and in particular its annual modulation, which occurs due to the Earth's motion, has been calculated for a range of analytic non-standard halo models [5,9–15]. It has been found that the region in the mass-cross section plane selected by the DAMA data depends substantially on the halo model assumed [10,12,15].

Analytic halo models usually assume an essentially static halo, whereas in reality the halo is forming via the ongoing infall of surrounding dark matter [16]. The caustic ring halo model, which arises from simple assumptions about the infall of dark matter onto the halo, provides an analytic model of some features of the dark matter distribution which may result from this accretion process. It is therefore worthwhile to calculate the observational features which the caustic ring halo model produces. The directional WIMP direct detection rate, which would be probed by proposed experiments such as the Directional Recoil Identification From Tracks (DRIFT) experiment [17], has been calculated by Copi, Han and Krauss [18], whilst Vergados [19] has calculated the total WIMP direct detection rate. In this paper we study the variation of the differential direct detection rate, in particular its annual modulation, with detector recoil energy.

II. CAUSTIC RING HALO MODEL

Cold dark matter (CDM) particles are collisionless and have low velocity dispersion ($<30\ \mathrm{km\,s^{-1}}$) so that particles falling onto an isolated galaxy are expected to oscillate in and out of the galaxy a number of times before they are virialized by inhomogeneities (such as molecular clouds, globular clusters and stars) [20]. These non-virialized CDM flows lead to the formation of caustic rings at the points where the particles with the most angular momentum in a given inflow reach their point of closest approach to the galactic center, hence the name of the model. Furthermore the distribution of the particles at any given location is expected to have a series of peaks in velocity space, corresponding to particles which are falling into the galaxy for the first time and those which have fallen in and out a number of times but have not yet been thermalized. Whilst this model is obviously a simplification of the hierarchical accretion process via which the galactic halo forms, in particular the Milky Way is not an isolated galaxy, the resolution of N-body simulations is not yet large enough to resolve these sorts of features.

The velocities and densities at the Earth's location expected due to these flows have been calculated using the self-similar infall model [21] generalized to take into account the angular momentum of the CDM particles [22]. The Earth is located between the 4th and 5th caustic rings and the velocity flows corresponding to these two rings constitute roughly 30% of the local halo density. Analysis of 32 extended galactic rotation curves has provided some evidence for the 1st and 2nd caustic rings [23], whilst analysis of an Infrared Astronomy Satellite (IRAS) map of the galactic disk apparently reveals the presence of the 5th ring [24].

The velocity distribution function of the velocity flows can be written as

TABLE I. The density and velocity components, in the rest frame of the galaxy, of the velocity flows.

j	ρ_j (10^{-26} g cm^{-3})	v_ϕ (km s^{-1})	v_z (km s^{-1})	v_r (km s^{-1})
1	0.4	140	±605	0
2	1.0	255	±505	0
3	2.0	350	±390	0
4	6.3	440	±240	0
5	9.2	440	0	±190
6	2.9	355	0	±295
7	1.9	290	0	±330
8	1.4	250	0	±350
9	1.1	215	0	±355
10	1.0	190	0	±355
11	0.9	170	0	±355
12	0.8	150	0	±350
13	0.7	135	0	±345
14	0.6	120	0	±340
15	0.6	110	0	±330
16	0.55	100	0	±325
17	0.50	90	0	±320
18	0.50	85	0	±310
19	0.45	80	0	±305
20	0.45	75	0	±300

$$f(\mathbf{v}) = \Sigma_j \rho_j \delta(\mathbf{v} - \mathbf{v}_j), \tag{1}$$

where ρ_j and $\mathbf{v}_j$ are the density and velocity of the j-th flow. Table I contains the most recently calculated values of ρ_j and $\mathbf{v}_j$ [25] (note that there are two, inward and outward, flows for each velocity peak). The total density is $\rho_0 = 102$ g cm$^{-3} = 0.57$ GeV cm^{-3}, with the velocity flows contributing 65% of the total. We will assume that the thermalized background distribution is a Maxwellian with velocity dispersion $v_0 = 220$ km s^{-1}.

III. ANNUAL MODULATION SIGNAL

The WIMP detection rate depends on the speed distribution of the WIMPs in the rest frame of the detector, f_v. This is found from the halo velocity distribution, $f(\mathbf{v})$ by making a Galilean transformation $\mathbf{v} \rightarrow \tilde{\mathbf{v}} = \mathbf{v} - \mathbf{v}_e$, where $\mathbf{v}_e$ is the Earth's velocity relative to the galactic rest frame, and then integrating over the angular distribution. In galactic coordinates the axis of the ecliptic lies very close to the $\phi - z$ plane and is inclined at an angle $\gamma \approx 29.80°$ to the $\phi - r$ plane. Including all components of the Earth's motion, not just that parallel to the galactic rotation [11]:

$$\mathbf{v}_e = v_1 \sin \alpha \hat{r} + (v_0 + v_1 \cos \alpha \sin \gamma) \hat{\phi} - v_1 \cos \alpha \cos \gamma \hat{z}, \tag{2}$$

where $v_0 \approx 232$ km s^{-1} is the speed of the sun with respect to the galactic rest frame, $v_1 \approx 30$ km s^{-1} is the orbital speed of the Earth around the Sun and $\alpha = 2\pi(t - t_0)/T$, with $T = 1$ year and $t_0 \sim 153$ days (June 2nd), when the component of the Earth's velocity parallel to the Sun's motion is largest.

In the range of masses and interaction cross sections accessible to current direct detection experiments the best motivated WIMP candidate is the neutralino, for which the event rate is dominated by the scalar contribution. The differential event rate simplifies to (see e.g. Refs. [7,15] for details)

$$\frac{dR}{dE} = \xi \sigma_p \left[\frac{\rho_{0.3}}{\sqrt{\pi} v_0} \frac{(m_p + m_\chi)^2}{m_p^2 m_\chi^3} A^2 T(E) F^2(E) \right], \tag{3}$$

where it is conventional to normalize the local WIMP density, ρ_χ, to a fiducial value $\rho_{0.3} = 0.3$ GeV cm^{-3}, such that $\xi = \rho_\chi / \rho_{0.3}$, E is the energy deposited in the detector, A is the atomic number of the detector nuclei, $F(E)$ is the detector form factor (the Saxon Woods form factor is used for I whilst that of Na is taken to be unity, see e.g. Ref. [10]) and $T(E)$ is defined as [7]

$$T(E) = \frac{\sqrt{\pi} v_0}{2} \int_{v_{min}}^{\infty} \frac{f_v}{v} dv, \tag{4}$$

where v_{min} is the minimum detectable WIMP velocity

$$v_{min} = \left(\frac{E(m_\chi + m_A)^2}{2 m_\chi^2 m_A} \right)^{1/2}, \tag{5}$$

m_χ is the WIMP mass and m_A is the atomic mass of the target nuclei.

In order to compare the theoretical signal with that observed we need to take into account the response of the detector. The electron equivalent energy, E_{ee}, which is actually measured is a fixed fraction of the recoil energy: $E_{ee} = q_A E$. The quenching factors for I and Na are $q_I = 0.09$ and $q_{Na} = 0.30$ respectively [26]. The energy resolution of the detector [9] is already taken into account in the data released by the DAMA Collaboration.

The expected experimental spectrum per energy bin for the DAMA Collaboration setup is then given by [10]

$$\frac{\Delta R}{\Delta E}(E) = r_{Na} \int_{E/q_{Na}}^{(E+\Delta E)/q_{Na}} \frac{dR_{Na}}{dE_{ee}}(E_{ee}) \frac{dE_{ee}}{\Delta E} + r_I \int_{E/q_I}^{(E+\Delta E)/q_I} \frac{dR_I}{dE_{ee}}(E_{ee}) \frac{dE_{ee}}{\Delta E}, \tag{6}$$

where $r_{Na} = 0.153$ and $r_I = 0.847$ are the mass fractions of Na and I respectively. Since $v_0 \gg v_1$ the differential event rate in the k-th energy bin can be expanded in a Taylor series in $\cos \alpha$ [6]:

$$\frac{\Delta R}{\Delta E}(E_k) \approx S_{0,k} + S_{m,k} \cos \alpha. \tag{7}$$

IV. RESULTS

Whilst all 3 components of the Earth's velocity need to be included to calculate the annual modulation signal accu-

TABLE II. The density, ϕ velocity component in the rest frame of the galaxy v_{ϕ}, ϕ velocity component in the rest frame of the Earth $\tilde{v}_{\phi}$, and total speed in the rest frame of the Earth $\tilde{v}_{\rm tot}$, of the caustic flows in June, when $\alpha=0$ (and in December when $\alpha=\pi$).

j	ρ_j (10^{-26} g cm^{-3})	v_{ϕ} (km s^{-1})	$\tilde{v}_{\phi}$ (km s^{-1})	$\tilde{v}_{\rm tot}$ (km s^{-1})
1	0.4	140	-104 (-78)	609(605)
2	1.0	255	11 (37)	50(506)
3	2.0	350	106 (132)	409(416)
4	6.3	440	196 (222)	310(327)
5	9.2	440	196 (222)	273(292)
6	2.9	355	111 (137)	311(321)
7	1.9	290	46 (72)	333(338)
8	1.4	250	6 (32)	350(351)
9	1.1	215	-29 (-3)	356(355)
10	1.0	190	-54 (-28)	359(356)
11	0.9	170	-74 (-48)	363(358)
12	0.8	150	-94 (-68)	362(357)
13	0.7	135	-109 (-83)	362(355)
14	0.6	120	-124 (-98)	362(354)
15	0.6	110	-134 (-108)	356(347)
16	0.55	100	-144 (-118)	355(346)
17	0.50	90	-154 (-128)	355(345)
18	0.50	85	-159 (-133)	348(337)
19	0.45	80	-164 (-138)	346(335)
20	0.45	75	-169 (-143)	344(332)

rately, the signal is largely determined by the component in the galactic plane [6]:

$$v_{e,\phi}=v_{\rm circ}[1.05+0.06\cos\alpha], \tag{8}$$

where $v_{\rm circ}=220$ km s^{-1} is the local circular velocity about the galactic center. Before presenting the results of a numerical calculation, using all three components of the Earth's velocity, we will carry out a simple analytic calculation, using only the component in the galactic plane, in order to elucidate the physical origin of the variation in $T(E)$.

In June, when $\alpha=0$,

$$v_{e,\phi}=1.11\times v_{\odot}=244.2 \ \ {\rm km\,s^{-1}}, \tag{9}$$

whilst in December, when $\alpha=\pi$,

$$v_{e,\phi}=0.99\times v_{\odot}=217.8 \ \ {\rm km\,s^{-1}}. \tag{10}$$

Table II contains the density, ϕ-velocity component, in the rest frames of the galaxy and Earth, and the total velocity in the rest frame of the Earth of the velocity flows for $\alpha=0$ and π. In both cases the total density in flows with negative v_{ϕ} (incident from the forward direction) is 17.1×10^{-26} g cm^{-3} whilst the total density in flows with positive v_{ϕ} (incident from the backward direction) is 49.4×10^{-26} g cm^{-3}, i.e., there are more WIMPs incident from backwards than forwards as found by Copi, Han and Krauss [18]. This is the opposite of the directional signal produced by a pure Maxwellian halo.

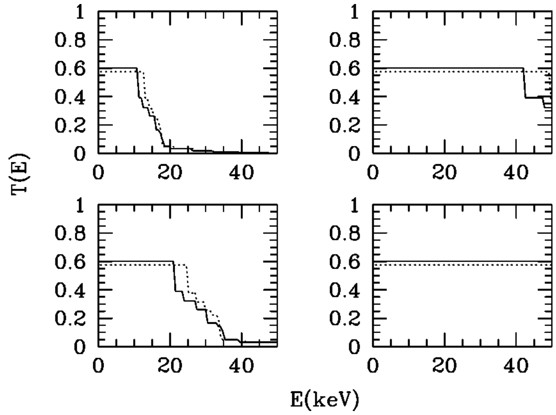

FIG. 1. The value of $T(E)$ in June (solid line) and December (dotted line) due to the velocity flows alone for four values of the WIMP mass $m_{\chi}=30,50,100,200$ GeV (top left, bottom left, top right and bottom right respectively).

In order to illustrate how the variations due to the caustics are smoothed out by the isothermal background we plot $T(E)$, as a function of E, for a Ge^{76} detector in Fig. 1 for the velocity flows alone, and in Fig. 2 for the complete halo model described above in Sec. II, where the velocity flows contribute 65% of the local density with the remaining 35% in an isothermal background. Values for other monatomic detectors can be found by rescaling the x axis by $m_{\rm A}/(m_{\rm A}+m_{\chi})^2$.

For a pure Maxwellian halo the signal is largest in December for small recoil energies, switching to become largest in June as the recoil energy is increased [13]. The signal for the velocity flows alone is more complicated. The contribution of the j-th velocity flow to $T(E)$ is proportional to $\rho_j/\tilde{v}_{\rm tot}$ if $\tilde{v}_{\rm tot}>v_{\rm min}$ and is zero otherwise. The contribution of the high density flows to the signal is largest in June, since their $\tilde{v}_{\rm tot}$ is smaller in June than in December. Therefore at low energies, where all the velocity flows contribute to the signal, the signal is largest in June. A given high density velocity flow stops contributing to the signal, $\tilde{v}_{\rm tot}<v_{\rm min}$, for

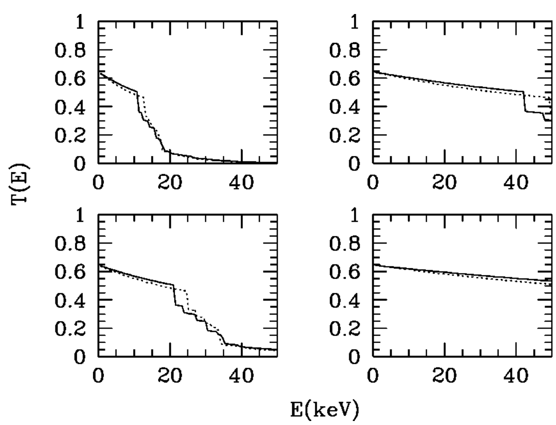

FIG. 2. The value of $T(E)$ in June (solid line) and December (dotted line) for a halo model with caustics plus an isothermal background, for four values of the WIMP mass $m_{\chi}=30,50,100,200$ GeV (as before).

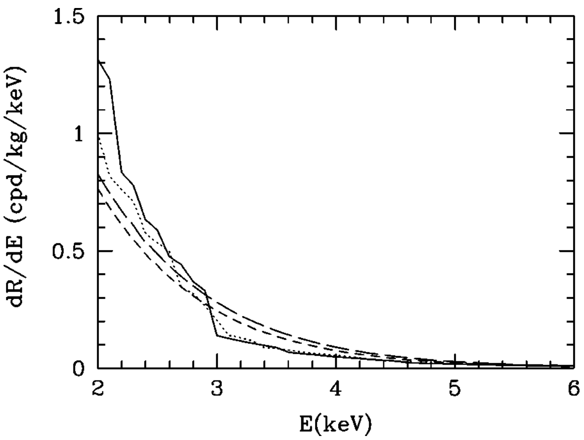

FIG. 3. The differential event rate dR/dE in June (solid line) and December (dotted line) for the caustic ring halo model with velocity flows plus a Maxwellian background as described in the text, and for a pure Maxwellian halo (June, long dashed line; December, short dashed line), for WIMP mass $m_{\chi}=54$ GeV and cross section $\xi\sigma_{\rm p}=4\times10^{-6}$ pb, as found by the DAMA Collaboration, for a NaI detector.

smaller $v_{\rm min}$, or equivalently E, in June compared to December however. This means that the steplike decreases in $T(E)$, which arise when a given flow stops contributing to the signal, occur at lower energies in June than in September (see Fig. 1). In other words for some range of recoil energies a given flow contributes to the signal in December but not in June. At large recoil energies only the low density flows, with high total velocity, can contribute and consequently the signal is far smaller than at low recoil energies. The lower density flows have negative $\tilde{v}_{\phi}$ and, in contrast to the high density flows, have larger speeds in June than in December, so that at high recoil energies the contribution due to a given flow is slightly larger in December. As m_{χ} is increased the variations in $T(E)$ are moved to higher E. The presence of a Maxwellian background smoothes the stepped variations in the signal produced by the flows, but they are still discernible and if detected would provide a distinctive indication of the presence of velocity flows.

In Fig. 3 we plot the differential event rate, dR/dE, for the velocity flows plus isothermal background model and also for a pure Maxwellian halo, for a NaI detector using the best fit values of the WIMP mass and cross section found by the DAMA Collaboration, $m_{\chi}=54$ GeV $\xi\sigma_{\rm p}=4\times10^{-6}$ pb.

Brhlik and Roszkowski [10] have devised a technique for comparing the experimental data released by DAMA with theoretical predictions for the annual modulation signal, in the absence of detailed information about the experimental setup, such as the efficiency of each NaI crystal. Their technique, which is effectively a least-squares comparison of the experimental data with the theoretical predictions, has been used to examine the region of mass–cross-section parameter space compatible with the DAMA results for various simple non-standard, but close to Maxwellian, halo models [10,15]. The best fit values and errors for $S_{0,\rm k}$ and $S_{\rm m,k}$ released by DAMA are calculated under the assumption that the recoil energy spectrum has the shape expected from a Maxwellian velocity distribution. Therefore whilst Brhlik and Roszkowski's technique can be used for halo models which produce recoil energy spectra close to that produced by a Maxwellian, it cannot be applied to the caustic flow model. Furthermore Gelmini and Gondolo have recently found that at low recoil energies the annual modulation produced by the flows is poorly approximated by a sinusoidal [27].

We can therefore only make a qualitative discussion of the effect of the presence of velocity flows on the DAMA allowed region. Brhlik and Roszkowski [10] found that, for a pure Maxwellian halo, the cutoff at large WIMP masses in the allowed region is determined by the time-dependent part of the signal (i.e., $S^{\rm th}_{\rm m,k}$), whilst the lower limit on the WIMP mass depends on both the time independent and dependent parts of the signal. When a velocity flow component is added to the Maxwellian background the recoil energy spectrum falls off less rapidly with increasing recoil energy for large WIMP masses, whilst for smaller WIMP masses the recoil energy spectrum falls off more rapidly with increasing energy (see Figs. 2 and 3). This suggests that the range of WIMP masses compatible with the energy distribution observed by DAMA would be likely to be smaller for the caustic ring model than for a pure Maxwellian halo. The allowed region obviously also depends on the magnitude and sign of the annual modulation. For the caustic flow model the sign of the modulation is opposite to that observed by DAMA for some, WIMP mass dependent, ranges of recoil energy, however since the experimental data is binned in 1 keV bins this may not prevent the velocity flow model being consistent with the DAMA data. It is possible though that the distinctive effects of the velocity flows on the recoil energy spectrum and on the sign of the annual modulation could lead to limits on the allowed fraction of the local halo density in velocity flows.

For the purpose of estimating WIMP direct detection rates the assumption of a standard Maxwellian halo is certainly reasonable. Now that experiments are reaching the region of parameter space populated by supersymmetric models, and in the case of DAMA claiming a positive signal, it is important to extend the theoretical analysis to more sophisticated, and hopefully more realistic, halo models. This process will be facilitated by the public release of data in a form subject to the minimum number of theoretical assumptions possible.

V. CONCLUSIONS

In this paper we have studied the WIMP direct detection signal, in particular its annual modulation, for the caustic ring halo model. In this model the WIMP distribution at the Earth's location has a series of peaks in velocity space, corresponding to particles which are falling into the galaxy for the first time and those which have fallen in and out a number of times but have not yet been thermalized. These peaks produce a distinctive imprint in the differential event rate, with the sign of the annual modulation (i.e. whether the event rate is larger in June or December) changing with detector recoil energy. The presence of an isothermal background component to the halo smoothes out the sharp changes in the differential event rate produced by the velocity flows but the distinctive changes in the sign of the annual modulation remain potentially discernible.

Finally we discussed the compatibility of this model with the results of the DAMA experiment. The recoil energy spectrum varies more rapidly with WIMP mass than that produced by a standard Maxwellian halo, whilst for some recoil energies the annual modulation signal has the opposite sign to that observed by DAMA. These effects suggest that for this model the region of WIMP mass–cross-section parameter space compatible with the DAMA data would be smaller than for the standard Maxwellian halo model. In addition it may be possible, via a full likelihood analysis, to constrain the fraction of the local halo density in velocity flows. This illustrates that if a significant component of the galactic dark matter is composed of WIMPs, then WIMP direct detection experiments with fine grained directional and energy resolution may be able to probe the local galactic structure, complementing the information which indirect detection experiments [28] would be able to provide on larger scales.

ACKNOWLEDGMENTS

A.M.G. was supported by PPARC and acknowledges use of the Starlink computer system at QMW. A.M.G thanks Craig Copi, Simon Goodwin and especially Pierre Sikivie for useful discussions.

[1] R. Bernabei *et al.*, Phys. Lett. B **389**, 757 (1996); **408**, 439 (1997); **424**, 195 (1998); **450**, 448 (1999).

[2] R. Bernabei *et al.*, Phys. Lett. B **480**, 23 (2000).

[3] G. Gerbier, J. Mallet, L. Mosca, and C. Tao, astro-ph/9710181; astro-ph/9902194.

[4] CDMS Collaboration, R. Abusaidi *et al.*, Nucl. Instrum. Methods Phys. Res. A **444**, 345 (2000); Phys. Rev. Lett. **84**, 5699 (2000).

[5] A. K. Drukier, K. Freese, and D. N. Spergel, Phys. Rev. D **33**, 3495 (1986).

[6] K. Freese, J. Frieman, and A. Gould, Phys. Rev. D **37**, 3388 (1988).

[7] G. Jungman, M. Kamionkowski, and K. Griest, Phys. Rep. **267**, 195 (1996).

[8] J. F. Navarro, C. S. Frenk, and S. D. M. White, Astrophys. J. **462**, 563 (1996); B. Moore *et al.*, Mon. Not. R. Astron. Soc. **310**, 1147 (1999); A. V. Kravtsov *et al.*, Astrophys. J. **502**, 48 (1998).

[9] F. Donato, N. Fornengo, and S. Scopel, Astropart. Phys. **9**, 247 (1998).

[10] M. Brhlik and L. Roskzkowski, Phys. Lett. B **464**, 303 (1999).

[11] J. D. Vergados, Phys. Rev. Lett. **83**, 3597 (1999); Phys. Rev. D **62**, 023519 (2000).

[12] P. Belli *et al.*, Phys. Rev. D **61**, 023512 (2000).

[13] P. Ullio and M. Kamionkowski, hep-ph/0006183.

[14] N. W. Evans, C. M. Carollo, and P. T. de Zeeuw, Mon. Not. R. Astron. Soc. **318**, 1131 (2000).

[15] A. M. Green, Phys. Rev. D **63**, 043005 (2001).

[16] J. E. Gunn and J. R. Gott, Astrophys. J. **176**, 1 (1972).

[17] M. Lehner *et al.*, proceedings of ''2nd International Conference on Dark Matter in Astro and Particle Physics,'' Heidelberg, 1998, astro-ph/9905074, pp. 767–771.

[18] C. J. Copi, J. Heo, and L. M. Krauss, Phys. Lett. B **461**, 43 (1999); C. J. Copi and L. M. Krauss, Phys. Rev. D **63**, 043507 (2001).

[19] J. D. Vergados, proceedings of ''NANPino-2000, Non Accelerator New Physics in Neutrino Observations,'' Dubna, Russia, hep-ph/0010151.

[20] J. R. Ipser and P. Sikivie, Phys. Lett. B **291**, 288 (1992).

[21] J. A. Filmore and P. Goldreich, Astrophys. J. **281**, 1 (1984); E. Bertschinger, Astrophys. J., Suppl. Ser. **58**, 39 (1985).

[22] P. Sikivie, I. I. Tkachev, and Y. Wang, Phys. Rev. Lett. **75**, 2911 (1995); Phys. Rev. D **56**, 1863 (1997).

[23] W. H. Kinney and P. Sikivie, Phys. Rev. D **61**, 087305 (2000).

[24] P. Sikivie (private communication).

[25] P. Sikivie, Nucl. Phys. B (Proc. Suppl.) **72**, 110 (1999).

[26] K. Fushimi *et al.*, Phys. Rev. C **47**, R425 (1993); G. J. Davies *et al.*, Phys. Lett. B **322**, 159 (1994); P. F. Smith *et al.*, *ibid.* **379**, 299 (1996).

[27] G. Gelmini and P. Gondolo, hep-ph/0012315.

[28] C. Calcaneo-Roldan and B. Moore, Phys. Rev. D **62**, 123005 (2000); L. Bergström, J. Edsjö, and C. Gunnarsson, *ibid.* **63**, 083515 (2001).